

MILD VELOCITY DISPERSION EVOLUTION OF SPHEROID-LIKE MASSIVE GALAXIES SINCE $Z \sim 2$

A. JAVIER CENARRO & IGNACIO TRUJILLO

Instituto de Astrofísica de Canarias, Vía Láctea s/n, 38200 La Laguna, Tenerife, Spain

Draft version March 26, 2009

ABSTRACT

Making use of public spectra from Cimatti et al. (2008), we measure for the first time the velocity dispersion of spheroid-like massive ($M_{\star} \sim 10^{11} M_{\odot}$) galaxies at $z \sim 1.6$. By comparing with galaxies of similar stellar mass at lower redshifts, we find evidence for a mild evolution in velocity dispersion, decreasing from $\sim 240 \text{ km s}^{-1}$ at $z \sim 1.6$ down to $\sim 180 \text{ km s}^{-1}$ at $z \sim 0$. Such mild evolution contrasts with the strong change in size (a factor of ~ 4) found for these type of objects in the same cosmic time, and it is consistent with a progressive larger role, at lower redshift, of the dark matter halo in setting the velocity dispersion of these galaxies. We discuss the implications of our results within the context of different scenarios proposed for the evolution of these massive objects.

Subject headings: galaxies: evolution — galaxies: formation — galaxies: structure — galaxies: kinematics and dynamics

1. INTRODUCTION

Recent observations show that the most massive ($M_{\star} \gtrsim 10^{11} M_{\odot}$) spheroid-like galaxies at $z > 1.5$, irrespective of their star formation activity (Pérez-González et al. 2008), were much smaller (a factor of ~ 4) than their local counterparts (Daddi et al. 2005; Trujillo et al. 2006, 2007; Longhetti et al. 2007; Zirm et al. 2007; Toft et al. 2007; Giavalisco et al. 2007; Ravindranath et al. 2008, Cimatti et al. 2008, hereafter C08; van Dokkum et al. 2008; Buitrago et al. 2008, hereafter B08; Saracco et al. 2009, Damjanov et al. 2009, Ferreras et al. 2009). The near absence of such systems ($r_e \lesssim 1.5 \text{ kpc}$; $M_{\star} \gtrsim 10^{11} M_{\odot}$) in the nearby Universe ($< 0.03\%$; Trujillo et al. 2009) implies a strong evolution in the structural properties of these massive galaxies as cosmic time evolves.

Different scenarios have been proposed to explain the dramatic size evolution of these galaxies since $z \sim 3$ (Khochfar & Silk 2006; Naab et al. 2007; Fan et al. 2008; Hopkins et al. 2009). The main difference among them is the role of mergers to increase the size of galaxies. Fan et al. (2008) support an evolutionary scheme where galaxies grow by the effect of quasar feedback, which removes huge amounts of cold gas from the central regions hence quenching the star formation. The removal of gas makes galaxies to puff up in an scenario similar to the one proposed to explain the growth of globular clusters (Hills 1980). In the merging scenario, however, merger remnants get larger sizes than those of their progenitors by transforming the kinetic energy of the colliding systems into potential energy. Whereas both scenarios predict a strong size evolution for the most massive galaxies, they disagree on the expected evolution of the velocity dispersion of the massive galaxies at a given stellar mass. The merging scenario basically predicts no evolution (at most a 30% since $z \sim 3$; Hopkins et al. 2009), whereas the puffing up scenario predicts central velocity dispersions to be ~ 2 times larger than in present-day massive galaxies.

Constraining the evolution of the velocity dispersion of spheroid-like massive galaxies over the last 10 Gyr turns

therefore crucial to test the above models of galaxy evolution, as well as to determine the importance of dark matter halos in setting the velocity dispersion of galaxies as cosmic time evolves. For these reasons, in this Letter we measure for the first time the velocity dispersion of such massive galaxies at $z \sim 1.6$, and compare it with a compilation of velocity dispersions for similar galaxies at $z \lesssim 1.2$. In what follows, we adopt a cosmology of $\Omega_m = 0.3$, $\Omega_{\Lambda} = 0.7$ and $H_0 = 70 \text{ km s}^{-1} \text{ Mpc}^{-1}$.

2. THE DATA

2.1. Velocity dispersions at $z \sim 1.6$

To determine the typical velocity dispersion of spheroid-like massive ($M_{\star} \sim 10^{11} M_{\odot}$) galaxies at $z \sim 1.6$, we have used the publicly available stacked spectrum of galaxies at $1.4 < z < 2.0$ ($\langle z \rangle = 1.63 \pm 0.18$ r.m.s. standard deviation) presented in C08 as part of the GMAS¹ (Galaxy Mass Assembly ultra-deep Spectroscopic Survey) project. The spectrum consists of an averaged spectrum of 13 massive galaxies with a total integration time of 480 h. Only 2 of them are classified as disks, whereas the remaining 11 galaxies have either a pure elliptical morphology or show a very concentrated and regular shape (see C08). The stacked spectrum is consequently representative of massive spheroid-like objects at that redshift. Individual galaxy spectra were taken at VLT with FORS2, using the grism G300I and a 1 arcsec width slit, providing a spectral resolution of FWHM $\sim 13 \text{ \AA}$ in the range $\lambda\lambda 6000 - 10000 \text{ \AA}$ ($\lambda/\Delta\lambda \sim 600$). Before stacking, each individual galaxy spectrum was previously de-redshifted and assigned to have the same weight in the $\lambda\lambda 2600 - 3100 \text{ \AA}$ rest-frame range. The resulting rest-frame stacked spectrum was set to $1 \text{ \AA}/\text{pix}$ over the range $\lambda\lambda 2300 - 3886 \text{ \AA}$.

Aimed at computing the velocity dispersion of the above stacked spectrum, it is required the use of reference template spectra of well known spectral resolution. Section 3.2 provides a full description of these data-sets, as they are basic input ingredients of the analysis carried out in this work.

Electronic address: cenarro@iac.es, trujillo@iac.es

¹ <http://www.arcetri.astro.it/cimatti/gmass/gmass.html>

2.2. Velocity dispersions up to $z \sim 1.2$

We have compiled from previous work velocity dispersions estimates of spheroid-like massive galaxies at $z < 1.2$. This includes data from van der Wel et al. (2005) —updated, when possible, with van der Wel et al. (2008)— for galaxies in the ranges $0.6 < z < 0.8$ and $0.9 < z < 1.2$, and from di Serego Alighieri et al. (2005) for galaxies at $0.9 < z < 1.3$. These authors also provide stellar masses and effective radii for their galaxies. In both samples the galaxies were classified visually. The vast majority of these objects present a prominent spheroidal component and are identified as either E or S0. When necessary, stellar masses have been transformed assuming a Chabrier (2003) IMF. To allow a meaningful comparison along the entire redshift interval explored in this paper, only galaxies with stellar masses in the range $0.5 < M_{\star} < 2 \times 10^{11} M_{\odot}$ have been considered.

To have a local reference, we have retrieved velocity dispersions, effective radii and stellar masses (Chabrier IMF) from the SDSS NYU Value-Added Galaxy Catalog (DR6; Blanton et al. 2005; Blanton & Roweis 2007) for those galaxies within the above stellar mass range having Sérsic (1968) indices (in the r-band) $n > 2.5$. Selecting objects with $n > 2.5$ assures that the majority of the sources have a Hubble morphological Type $T < 0$ (i.e. ranging from E to S0; Ravindranath et al. 2004). We have estimated the average velocity dispersion of the above galaxies in two redshift bins: $0 < z < 0.1$ and $0.1 < z < 0.2$. We have not tried higher redshifts to assure individual signal-to-noise ratios (S/N) larger than 10.

3. VELOCITY DISPERSION COMPUTATION

3.1. The MOVEl program

To estimate the velocity dispersion of the C08 stacked spectrum we use the MOVEl code, available at the REDUCEME² distribution (Cardiel 1999). MOVEl is designed to characterize the line-of-sight velocity distribution of a galaxy spectrum by determining its first two moments: the mean radial velocity and the velocity dispersion. Based on Fourier analysis, the code relies on the MOVEl and OPTEMA algorithms of González (1993). A full explanation of the Fourier techniques and their particular implementation in both routines is provided in the above work.

The MOVEl algorithm, an improvement of the classic Fourier quotient method by Sargent et al. (1977), is an iterative procedure in which a galaxy model is processed in parallel to the galaxy spectrum. In this way, a comparison between the input and recovered broadening functions for the model allows to correct the galaxy power spectrum from any imperfections of the data handling in Fourier space. The OPTEMA algorithm is designed to overcome the typical template mismatch problem by computing an optimal template for the galaxy spectrum. It is fed with a set of representative template spectra which are scaled, shifted and broadened according to initial values for the mean line strength, the radial velocity, and the velocity dispersion. Then, the algorithm finds the linear combination of the template spectra that best matches the observed galaxy spectrum. This constitutes a first

composite template which is fed into the MOVEl algorithm. The output kinematic parameters are then used to create an improved composite template and the process is iterated until it converges. This iterative approach then provides an optimal template while simultaneously computing the radial velocity and velocity dispersion of the galaxy spectrum.

Ideally, the reference template spectra are chosen to be representative stellar spectra observed with an identical technical setup to that of the galaxy spectra. This way, the instrumental broadening is the same in both data sets, and the broadening difference between galaxy and template spectra, $\Delta\sigma$, is a direct measurement of the galaxy starlight velocity dispersion, σ_{\star} . Since this is not the case for the C08 stacked spectrum, the different instrumental resolutions of the distinct data sets employed in this work must be taken into account. This is explained in detail in Sections 3.2 and 3.3.

3.2. The template spectra

We have restricted the kinematical analysis of the C08 spectrum to those regions containing strong spectral features from the galaxy starlight. Because of the lack of available template spectra of high-enough spectral resolution covering the full spectral range of interest, we employ three different data sets. Two of them allow us to analyze the near ultraviolet (NUV) region at $\lambda \leq 3050 \text{ \AA}$, which comprises e.g. several FeII lines at $\lambda \sim 2600 \text{ \AA}$, the $\lambda 2800 \text{ MgII}$ doublet and the $\lambda 2852 \text{ MgI}$ line. The third template set is chosen to provide a complementary analysis from the region $\lambda \geq 3250 \text{ \AA}$, with features such as the $\lambda 3360 \text{ NH}$ and $\lambda 3862 \text{ CNO}$ bands. The three sets of template spectra, whose properties are summarized in Table 1, are described below:

i) First, from the CoolCAT³ database, an HST/STIS echelle catalog of normal late-type stars with $R \sim 40000$ (Ayres 2005), we have selected eight spectra (from F5V to G0III spectral types) covering the range $\lambda 2510 - 3050 \text{ \AA}$ with no gaps in between. They have been rebinned at $1 \text{ \AA}/\text{pix}$ to match the linear dispersion of the C08 spectrum. Using MOVEl and their corresponding high-resolution CoolCAT spectra as reference templates, we have derived that the spectral resolution of the rebinned templates is $\sigma_{\text{STIS}} \sim 57 \pm 3 \text{ km s}^{-1}$ at $\lambda \sim 2800 \text{ \AA}$, which corresponds to $R \sim 2240$.

ii) The second set of template spectra consists of a subsample of nineteen SSP spectral energy distributions by G. Bruzual (private communication). They are based on the Bruzual & Charlot (2003) code and the Next Generation Spectral Library, NGSL (Gregg et al. 2004; Heap & Lindler 2007), with an average resolution of $R \sim 1000$. The employed SSP models span ages from 0.3 to 3 Gyr with metallicities $[Z/H] = -0.4, 0.0, \text{ and } +0.4$, hence enclosing the 1 Gyr and solar metallicity estimate of C08 for their stacked spectrum. Again, using MOVEl and the above high-resolution CoolCAT spectra, we have accurately derived the spectral resolution of Bruzual's models in the range $\lambda 2510 - 3050 \text{ \AA}$, which is $\sigma_{\text{BC03+NGSL}} \sim 178 \pm 8 \text{ km s}^{-1}$, or equivalently $R \sim 710$.

iii) Finally, for the red side of the C08 stacked spectrum, we employ a set of eighteen stellar spectra (dwarfs

² <http://www.ucm.es/info/Astrof/software/reduceme/reduceme.html>

³ <http://casa.colorado.edu/~ayres/CoolCAT/>

TABLE 1
VELOCITY DISPERSION ESTIMATES FOR SPHEROID-LIKE MASSIVE GALAXIES AT $z \sim 1.6$

Template spectra	Spectral range (\AA) ^a	λ_c (\AA) ^b	$\sigma_{0,\text{templ}}$ (km s^{-1}) ^c	$\sigma_{0,\text{C08}}$ (km s^{-1}) ^d	$\Delta\sigma$ (km s^{-1}) ^e	$\sigma_{*,\text{C08}}$ (km s^{-1}) ^f
CoolCAT stars	2510 – 3050	2780	57 ± 3	230	267 ± 20	258 ± 21
BC03+NGSL SSP models	2510 – 3050	2780	178 ± 8	230	178 ± 23	236 ± 18
Keck/LRIS stars	3250 – 3880	3565	171 ± 5	179	177 ± 20	236 ± 15

^a Rest-frame spectral range employed for deriving the MOVEl kinematics ($\Delta\sigma$)^b Central wavelength of the rest-frame spectral range^c Instrumental resolution of the template spectra computed at λ_c (see text in Section 3.2).^d Instrumental resolution of the C08 stacked spectrum computed at λ_c , using $\text{FWHM} = 13 \text{\AA}$ and $z = 1.6$.^e Relative velocity dispersion with respect to that of the optimal template spectra.^f Velocity dispersion of the C08 stacked spectrum of spheroid-like massive galaxies at $z \sim 1.6$, as derived from Equation. 1.

and giants ranging from G0 to K7 spectral types) observed with LRIS at Keck as radial velocity templates for a different program (Beasley et al. 2009). Having used the grism 600/4000 and the 1 arcsec longslit, the stellar spectra have a FWHM of $4.77 \pm 0.14 \text{\AA}$ ($\sigma_{\text{LRIS}} \sim 171 \pm 5 \text{ km s}^{-1}$ at 3565\AA ; $R \sim 750$) as determined from the width of the wavelength calibration arc lines. The spectra span the range $\lambda\lambda 3150 - 5600 \text{\AA}$, although only the blue side is employed here.

3.3. Results and robustness of the method

We have analyzed the stacked spectrum of C08 with MOVEl using the three sets of template spectra described in Section 3.2. In each case, to constrain the reliability of the final results, the procedure has been repeated several times using different initial MOVEl parameters, like e.g. different starting velocity dispersions (from 50 up to 300 km s^{-1} , in steps of 50 km s^{-1}).

For each single MOVEl solution, the stellar velocity dispersion of the C08 stacked spectrum, $\sigma_{*,\text{C08}}$, is derived as

$$\sigma_{*,\text{C08}} = \sqrt{\Delta\sigma^2 + \sigma_{0,\text{templ}}^2 - \left(\frac{\sigma_{0,\text{C08}}}{1+z}\right)^2}, \quad (1)$$

where $\Delta\sigma$ is the broadening difference between the optimal template spectra and the C08 spectrum (as derived from MOVEl), $\sigma_{0,\text{templ}}$ and $\sigma_{0,\text{C08}}$ are their intrinsic instrumental resolutions, and z is the redshift (~ 1.6). Note that, since the individual galaxy spectra of C08 were previously blue-shifted before stacking, the effective instrumental resolution at rest-frame decreases by $(1+z)$.

For each set of template spectra, Table 1 presents $\sigma_{0,\text{templ}}$, $\sigma_{0,\text{C08}}$, and the mean values of $\Delta\sigma$ and $\sigma_{*,\text{C08}}$, with their errors accounting for the r.m.s. standard deviation of the solutions obtained from the different MOVEl trials. An error-weighted mean of the three independent $\sigma_{*,\text{C08}}$ solutions, which are indeed consistent within the uncertainties, gives $\langle\sigma_{*,\text{C08}}\rangle = 241 \pm 10 \text{ km s}^{-1}$.

It is worth noting that the above value could be slightly overestimated, as redshift uncertainties for the 13 stacked galaxy spectra may have enlarged artificially the width of the lines. We have also checked that the strong $\lambda 2800 \text{ MgII}$ doublet in the stacked spectrum ($\sim 8 \text{\AA}$, Table 2 of C08) is not significantly broadened by potential non-stellar MgII absorptions in surrounding galactic gas clouds. Such absorptions are typically much narrower ($\sim 45 \text{ km s}^{-1}$, as they follow much colder kinematics) and ~ 5 times weaker ($\sim 1.6 \text{\AA}$, for typically ~ 14 clouds; see e.g. Steidel et al. 1994; Churchill et al. 2000). Therefore, even if they were present in all galaxies,

$\langle\sigma_{*,\text{C08}}\rangle$ could be overestimated by only $\sim 1 \text{ km s}^{-1}$ (up to $\sim 14 \text{ km s}^{-1}$ if all galaxies were Damped- $\text{Ly}\alpha$ systems, which is very unlikely as no Lyman absorptions are detected). On the other hand, if the two disk galaxies in the stacked spectrum had lower typical velocity dispersions of e.g. 150 km s^{-1} , the derived $\langle\sigma_{*,\text{C08}}\rangle$ would underestimate the true velocity dispersion of early-type galaxies by $\sim 13 \text{ km s}^{-1}$. Overall, since the above systematics may cancel each other, $241 \pm 10 \text{ km s}^{-1}$ is probably a reasonable estimation of the velocity dispersion of $M_* \sim 10^{11} M_\odot$ spheroid-like galaxies at $z \sim 1.6$.

Figure 1 illustrates representative MOVEl solutions as derived from each template set. At the NUV, CoolCAT stars (panel *a*) provide a slightly more broadened solution than the NGSL-based SSP models (panel *b*), probably due to the intrinsic differences between the two template sets and their effects on the template mismatch problem. At longer wavelengths (panel *c*), the galaxy spectral features look somewhat blurred, probably by sky line residuals commonplace of the near-infrared region at observed frame. Still, in all cases the solutions reproduce nicely the C08 spectrum.

To further check the reliability of the MOVEl results, we carried out Monte Carlo simulations in which we added Gaussian noise (to match $\text{S/N} = 5$ to 30\AA^{-1}) to artificially broadened reference template spectra ($\Delta\sigma = 100 - 400 \text{ km s}^{-1}$, in steps of 50 km s^{-1}) from our three template sets. For such *fake* galaxy spectra, we run the MOVEl procedure in the same way as we did for the C08 stacked spectrum. As expected, the accuracy in the final solution decreases with the decreasing S/N of the problem spectrum. The typical scatter of the derived $\Delta\sigma$ solutions —averaged over all the simulations and initial MOVEl conditions— are 55 , 24 , 12 , and 8 km s^{-1} for $\text{S/N} = 5$, 10 , 20 , and 30\AA^{-1} respectively. More importantly, for all S/N values, the recovered mean $\Delta\sigma$ is statistically consistent with the assumed input value, hence supporting the reliability of both the method and $\sigma_{*,\text{C08}}$.

4. DISCUSSION

The fact that the velocity dispersion of $M_* \sim 10^{11} M_\odot$ spheroid-like galaxies at $z \sim 1.6$ is $\sim 240 \text{ km s}^{-1}$ has important consequences to understand their evolution:

- It confirms that high- z spheroid-like massive galaxies are truly massive objects. The unexpected strong size evolution of these objects has cast some doubts about the reliability of their stellar mass estimates, which relies on the assumption that the IMF is the same at all redshifts. In fact, an appropriate change of the IMF with redshift would

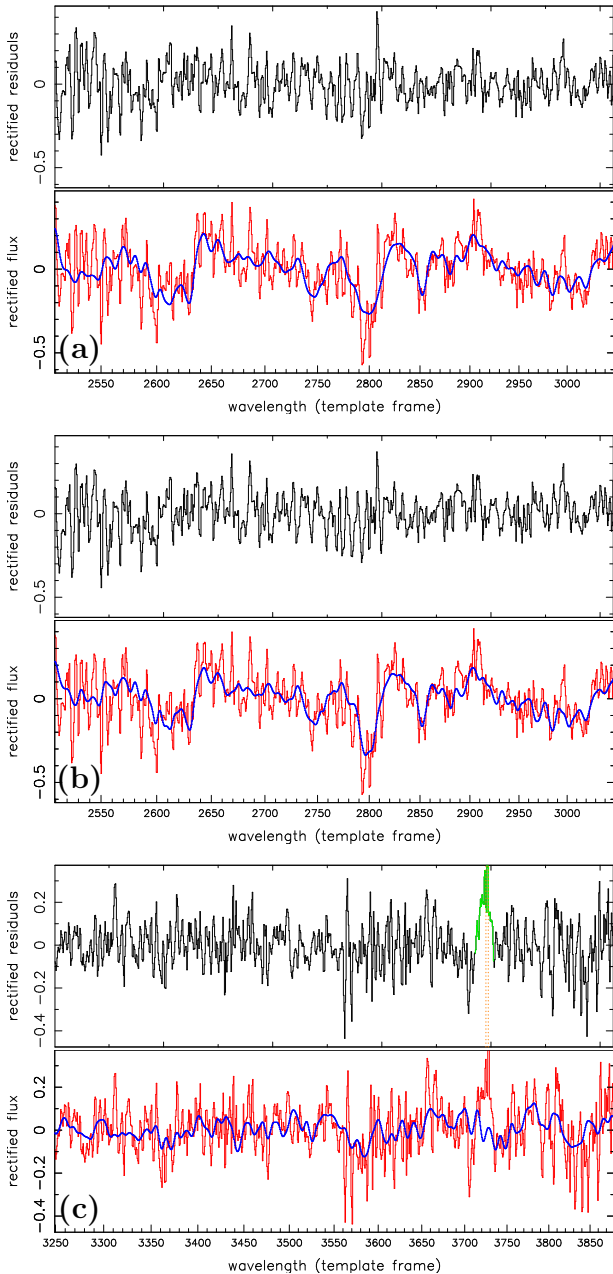


FIG. 1.— Representative examples of the MOVEL fitting results derived for the C08 stacked spectrum and the three sets of template spectra: (a) CoolCAT stars, (b) BC03+NGSL SSP models, and (c) Keck/LRIS stars. In each case, bottom panels illustrate the C08 stacked spectrum of galaxies at $z \sim 1.6$ (red) and the optimal template spectrum (blue, thick line) broadened at the mean $\Delta\sigma$ values in Table 1. Top panels show the residuals of the fits. In panel c, the region around the OII emission line doublet at $\lambda 3727 \text{ \AA}$ (dotted lines) was masked and rejected from the C08 stacked spectrum (green) for the fitting computation.

mitigate the problem of the strong size evolution. However, the derived velocity dispersion at $z \sim 1.6$ is similar to that of present-day galaxies with $M_* > 10^{11} M_\odot$, consequently constraining any potential change of the IMF with redshift.

- It alleviates the problem of understanding how massive—and compact—galaxies at high- z can evolve through merging since that epoch. An extraordinarily high velocity dispersion at high- z (e.g. $\sim 400 \text{ km s}^{-1}$) would have implied that the

gravitational potential depth of the system would be so intense that it would not easily evolve in size.

To put in context the above result, Figure 2 shows the sizes (top panel) and velocity dispersions (bottom panel) for the C08 galaxies and the compilation of spheroid-like galaxies of similar mass described in Section 2. These galaxies follow nicely the observed strong size evolution found in other independent larger samples where completeness effects are accounted (Trujillo et al. 2007; B08; dashed line), hence probing that the sizes of the objects explored in this paper are typical of average spheroidal-like massive galaxies at those redshifts. It is also clear that, although massive spheroid-like galaxies have experienced a strong size evolution (a factor of ~ 4 since $z \sim 1.5$; Trujillo et al. 2007), the velocity dispersion has evolved mildly by a factor of ~ 1.3 in the same redshift interval (see Bernardi 2009 for a similar trend at $z < 0.3$). This result is crucial to constrain the different scenarios proposed so far to explain the dramatic size evolution since $z \sim 2$, as they disagree in the amount of evolution expected in their velocity dispersions.

In the puffing up scenario of Fan et al. (2008), velocity dispersions change as $\sigma_* \propto r_e^{-1/2}$. Using the observed size evolution of B08, $r_e(z) \propto (1+z)^{-1.48}$, the solid line in Fig. 2 illustrates the expected σ_* evolution under this scenario. It increases with redshift in a way that galaxies are expected to double their σ_* at $z \sim 1.5$. The observed velocity dispersions are compatible—within the error bars—with this scenario up to $z \sim 0.7$. However, at $z > 1$ the discrepancy between theory and data is apparent.

In the merging scenario of Hopkins et al. (2009), at a fixed stellar mass, σ_* evolves with redshift as

$$\frac{\sigma_*(z)}{\sigma_*(0)} \propto \frac{1}{\sqrt{1+\gamma}} \sqrt{\gamma + \frac{r_e(0)}{r_e(z)}}, \quad (2)$$

where $\gamma \equiv (M_{\text{halo}}/R_{\text{halo}})/(M_*/r_e)$ is the dark matter contribution to the central potential relative to that of the baryonic matter at $z \sim 0$, and R_{halo} is the effective radius of the halo. Again, we have used the B08 size evolution as an input into the merging model prediction. The grey area in Fig. 2 encloses the expected σ_* evolution when γ varies between 1 and 2. The agreement between the merging scheme and the observed evolution looks reasonably good at all redshifts.

Following Hopkins et al. (2009), to explain why σ_* has only changed weakly since $z \sim 2$ it is necessary to consider that the observed velocity dispersion is driven by two components: the baryonic matter and the dark matter halo. Both components contribute linearly to the central gravitational potential of the galaxy, hence $\sigma_* \propto (M_*/r_e + M_{\text{halo}}/R_{\text{halo}})$. Assuming that R_{halo} evolves weakly with time (most simulations show that halos build inside-out, so the central potential is set first and just the outer halo grows with time), the dark matter effect on the central potential of the galaxy (i.e. on σ_*) basically remains unchanged at a fixed M_* . However, the influence of the baryonic matter on the gravitational potential has changed strikingly since $z \sim 1.5$, at present-day being ~ 4 times smaller due to the expansion of the object. The relative influence of the dark matter on setting the inner potential increases with the decreasing effect of the baryonic matter. In fact, the data look in

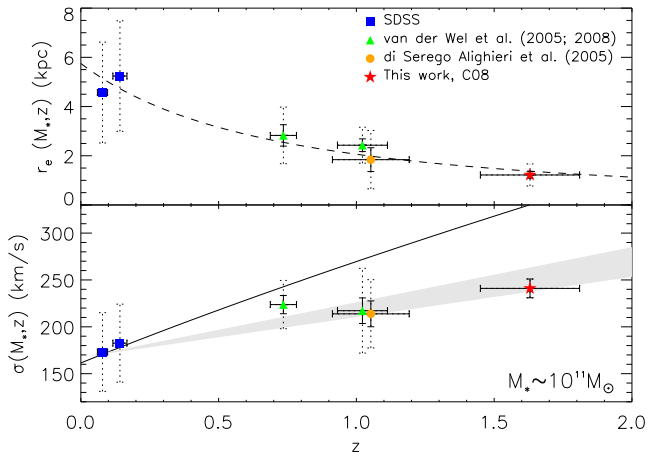


FIG. 2.— *Top Panel:* Size evolution of $M_* \sim 10^{11} M_\odot$ spheroid-like galaxies as a function of redshift. Different symbols show the median values of the effective radii for the different galaxy sets considered in this work (see Section 2), as indicated in the labels. Dashed error bars, if available, show the dispersion of the sample, whereas the solid error bars indicate the uncertainty of the median value. The dashed line represents the observed evolution of sizes $r_e(z) \propto (1+z)^{-1.48}$ found in B08 for galaxies of similar stellar mass. *Bottom Panel:* Velocity dispersion evolution of the spheroid-like galaxies as a function of redshift, with symbols as given above. Assuming the B08 size evolution, the solid line represents the prediction from the “puffing up” scenario (Fan et al. 2008), whereas the grey area illustrates the velocity dispersion evolution within the merger scenario of Hopkins et al. (2009) for $1 < \gamma < 2$. See text for details.

agreement with an almost symmetric influence of dark and baryonic matter (i.e. $\gamma \sim 1$) in setting the central gravitational potential of present-day objects.

We acknowledge the referee for constructive comments. This work has been possible thanks to the helpful contribution of several people. G. Bruzual provided us with his SSP model predictions based on the NGSL. Fruitful discussions with P. Sánchez-Blázquez, A. Vazdekis and C. Conselice helped us to find the right strategy to achieve our goals. N. Cardiel gave us very valuable inputs on the MOVELE capabilities. Finally, we benefited from discussion with R. Guzmán, M. Balcells, M. López-Corredoira, and A. van der Wel. A.J.C. and I.T.C. are Juan de la Cierva and Ramón y Cajal Fellows of the Spanish Ministry of Science and Innovation. This work has been funded by the Spanish Ministry of Science and Innovation through grant AYA2007-67752-C03-01.

REFERENCES

- Ayres, T. R. 2005, 13th Cambridge Workshop on Cool Stars, Stellar Systems and the Sun, 560, 419
- Beasley, M. A., Cenarro, A. J., Strader, J., & Brodie, J. P. 2009, AJ, accepted, astro-ph.
- Bernardi, M. 2009, arXiv:0901.1318
- Blanton, M. R., et al. 2005, AJ, 129, 2562
- Blanton, M. R., & Roweis, S. 2007, AJ, 133, 734
- Bruzual, G., & Charlot, S. 2003, MNRAS, 344, 1000
- Buitrago, F., Trujillo, I., Conselice, C. J., Bouwens, R. J., Dickinson, M., & Yan, H. 2008, ApJ, 687, L61 (B08)
- Cardiel, N. 1999, Ph.D. Thesis, Universidad Complutense de Madrid
- Chabrier, G. 2003, PASP, 115, 763
- Churchill, C. W., Mellon, R. R., Charlton, J. C., Jannuzi, B. T., Kirhakos, S., Steidel, C. C., & Schneider, D. P. 2000, ApJ, 543, 577
- Cimatti et al. 2008 A&A, 482, 21 (C08)
- Daddi, E., et al. 2005, ApJ, 626, 680
- Damjanov, I., et al. 2008, arXiv:0807.1744
- di Serego Alighieri, S., et al. 2005, A&A, 442, 125
- Fan, L., Lapi, A., De Zotti, G., & Danese, L. 2008, ApJ, 689, L101
- Ferreras, I., Lisker, T., Pasquali, A., Khochfar, S., Kaviraj, S., 2009, arXiv:0901.4555
- Gregg, M. D., et al. 2004, Bulletin of the American Astronomical Society, 36, 1496
- Giavalisco, M., Ravindranath, S., Daddi, E., 2007, NCimB, 122, 1209
- González, J. J., 1993, PhDT, University of California
- Heap, S. R., & Lindler, D. J. 2007, From Stars to Galaxies: Building the Pieces to Build Up the Universe, 374, 409
- Hills, J. G. 1980, ApJ, 235, 986
- Hopkins, P. F., Hernquist, L., Cox, T. J., Keres, D., & Wuyts, S. 2009, ApJ, 691, 1424
- Khochfar, S., & Silk, J. 2006, ApJ, 648, L21
- Longhetti, M., et al. 2007, MNRAS, 374, 614
- Naab, T., Johansson, P. H., Ostriker, J. P., & Efstathiou, G. 2007, ApJ, 658, 710
- Pérez-González, P. G., Trujillo, I., Barro, G., Gallego, J., Zamorano, J., Conselice, C. J., 2008, ApJ, 687, 50
- Ravindranath, S., et al. 2004, ApJ, 604, L9
- Ravindranath, S., Daddi, E., Giavalisco, M., Ferguson, H. C., Dickinson, M. E., 2008, IAUS, 245, 407
- Saracco, P., Longhetti, M., & Andreon, S. 2009, MNRAS, 392, 718
- Sargent, W. L. W., Schechter, P. L., Boksenberg, A., & Shorridge, K. 1977, ApJ, 212, 326
- Sersic, J. L. 1968, Cordoba, Argentina: Observatorio Astronomico, 1968,
- Steidel, C. C., Dickinson, M., & Persson, S. E. 1994, ApJ, 437, L75
- Toft, S., et al. 2007, ApJ, 671, 285
- Trujillo, I., et al. 2006, MNRAS, 373, L36
- Trujillo, I., Conselice, C. J., Bundy, K., Cooper, M. C., Eisenhardt, P., & Ellis, R. S. 2007, MNRAS, 382, 109
- Trujillo, I., Cenarro, A. J., de Lorenzo-Caceres, A., Vazdekis, A., de la Rosa, I. G., & Cava, A. 2009, ApJ, 692, L118
- van der Wel, A., Franx, M., van Dokkum, P. G., Rix, H.-W., Illingworth, G. D., & Rosati, P. 2005, ApJ, 631, 145
- van der Wel, A., Holden, B. P., Zirm, A. W., Franx, M., Rettura, A., Illingworth, G. D., & Ford, H. C. 2008, ApJ, 688, 48
- van Dokkum, P. G., et al. 2008, ApJ, 677, L5
- Zirm, A. W., et al. 2007, ApJ, 656, 66